

Quantum Zeno effect versus adiabatic quantum computing and quantum annealing

Naser Ahmadianiaz,¹ Dennis Kraft,¹ Gernot Schaller,¹ and Ralf Schützhold^{1,2}

¹*Helmholtz-Zentrum Dresden-Rossendorf, Bautzner Landstraße 400, 01328 Dresden, Germany*

²*Institut für Theoretische Physik, Technische Universität Dresden, 01062 Dresden, Germany*

(Dated: September 5, 2025)

For the adiabatic version of Grover's quantum search algorithm as proposed by Roland and Cerf, we study the impact of decoherence caused by a rather general coupling to some environment. For quite generic conditions, we find that the quantum Zeno effect poses strong limitations on the performance (quantum speed-up) since the environment effectively measures the state of the system permanently and thereby inhibits or slows down quantum transitions. Generalizing our results, we find that analogous restrictions should apply universally to adiabatic quantum algorithms and quantum annealing schemes which are based on isolated Landau-Zener type transitions at avoided level crossings (similar to first-order phase transitions). As a possible resort, more gradual changes of the quantum state (as in second-order phase transitions) or suitable error-correcting schemes such as the spin-echo method may alleviate this problem.

I. INTRODUCTION

A. Quantum Zeno Effect

The Greek philosopher Zeno (or Zenon) formulated several apparent paradoxes illuminating the tension between the two concepts of being in motion versus being at a certain position at a given time. As a famous example, imagine a race between the fast Achilles and a slow tortoise where both start at the same time but the tortoise gets a head start. Then, before being able to overtake the tortoise, Achilles must first reach the place where the tortoise started – but, during that time, the tortoise already moved away and covered an additional distance. Thus, Achilles needs some more time to cover this distance too, which allows the tortoise to move even further, and so on. This leads to a never ending sequence such that one might expect that Achilles should never be able to overtake the tortoise.

Intriguingly, this apparent paradox resurges in quantum theory [1–10] where frequent measurements of the state of a system (corresponding to the concept of position) may slow down or even inhibit the quantum evolution in the form of a transition to another state (corresponding to the concept of motion). As a simple example, let us consider the unitary evolution of a spin-1/2 system $|\psi(t)\rangle$ which rotates $|\psi(t)\rangle = \cos(\Omega t) |\uparrow\rangle + \sin(\Omega t) |\downarrow\rangle$ from the initial state $|\uparrow\rangle$ to the final state $|\downarrow\rangle$. Measuring the state of the system (in the $|\uparrow\rangle, |\downarrow\rangle$ basis) after a short time $\Delta t \ll 1/\Omega$ projects it to one of the basis states with the probabilities $P_\uparrow = \cos^2(\Omega\Delta t)$ or $P_\downarrow = \sin^2(\Omega\Delta t) \approx (\Omega\Delta t)^2$. Repeating this measurement N times with $N\Omega\Delta t = \pi/2$ then yields the total transition probability $1 - \cos^{2N}(\Omega\Delta t)$ which scales as $N(\Omega\Delta t)^2 \ll 1$, i.e., the transition rate is strongly reduced from $\mathcal{O}(\Omega)$ to $\mathcal{O}(\Omega^2\Delta t)$. As one way to understand this reduction, we have to sum small probabilities (in the case of measurements) instead of small amplitudes (for unitary evolution).

Besides the projective measurements discussed above,

weak measurements [11, 12] can have a similar effect [13, 14] – provided that the system dynamics is slow enough. In order to illustrate this point, let us consider the standard Lindblad master equation ($\hbar = 1$)

$$\frac{d\hat{\rho}}{dt} = -i [\hat{H}, \hat{\rho}] + \hat{L}\hat{\rho}\hat{L}^\dagger - \frac{1}{2} \{ \hat{L}^\dagger \hat{L}, \hat{\rho} \}, \quad (1)$$

where the system Hamiltonian \hat{H} generates the unitary time evolution of the density matrix $\hat{\rho}$ while the Lindblad (jump) operator \hat{L} describes the impact of the environment, which may cause a non-unitary time evolution.

Choosing a spin-1/2 system with $\hat{H} = \Omega\hat{\sigma}_y$, the unitary system dynamics itself (i.e., for $\hat{L} = 0$) would correspond to the rotation between the states $|\uparrow\rangle$ and $|\downarrow\rangle$ as described above. Now let us add the Lindblad operator $\hat{L} = \sqrt{\Gamma}\hat{\sigma}_z$ which generates decoherence with the damping rate Γ and leads to a decay of the coherences between the states $|\uparrow\rangle$ and $|\downarrow\rangle$, i.e., the off-diagonal matrix elements of $\hat{\rho}$ in the $|\uparrow\rangle, |\downarrow\rangle$ basis (phase damping). Then the evolution equation for the expectation value of the spin operator $\langle\hat{\sigma}\rangle$ reads

$$\frac{d}{dt}\langle\hat{\sigma}\rangle = -2\mathbf{\Omega} \times \langle\hat{\sigma}\rangle + 2\mathbf{L} \times (\mathbf{L} \times \langle\hat{\sigma}\rangle), \quad (2)$$

with $\mathbf{\Omega} = \Omega\mathbf{e}_y$ and $\mathbf{L} = \sqrt{\Gamma}\mathbf{e}_z$. For $\Omega \gg \Gamma$, we approximately find rotation with a frequency Ω which slowly decays with a damping rate of $\mathcal{O}(\Gamma)$. For $\Omega \ll \Gamma$, on the other hand, the rotation disappears and we find a slow decay to the fully mixed state $\hat{\rho} = \mathbf{1}/2$ (with $\mathbf{1}$ denoting the unit matrix) on a long time scale of $\mathcal{O}(\Gamma/\Omega^2)$. As an intuitive picture, the environment measures the state of the system with an effective measurement rate $\Gamma \sim 1/\Delta t$. Thus, the slow decay to $\hat{\rho} = \mathbf{1}/2$ with the decay rate $\mathcal{O}(\Omega^2/\Gamma)$ corresponds to the example above with the reduced transition rate $\mathcal{O}(\Omega^2\Delta t)$. Note that analogous results can be obtained for Lindblad operators in the form of projectors $\hat{L} = \sqrt{\Gamma}\hat{P}_1$ or $\hat{L} = \sqrt{\Gamma}\hat{P}_2$ or a combination of both $\hat{L}_1 = \sqrt{\Gamma_1}\hat{P}_1$ and $\hat{L}_2 = \sqrt{\Gamma_2}\hat{P}_2$, see Appendix A. Furthermore, in App. B we also provide an example of Zeno freezing in the strong-coupling regime that does not require a Lindblad treatment.

B. Adiabatic Quantum Algorithms

In contrast to the usual scheme of sequential quantum algorithms [15] where the desired final state $|\psi_{\text{out}}\rangle$ is obtained by applying a sequence of quantum gates onto some initial state $|\psi_{\text{in}}\rangle$, adiabatic quantum algorithms [16–18] encode the solution to the problem of interest into the ground state of a suitably chosen Hamiltonian \hat{H}_{out} . In order to reach this final ground state $|\psi_{\text{out}}\rangle$, the idea is to start with an initial Hamiltonian \hat{H}_{in} whose ground state $|\psi_{\text{in}}\rangle$ is known and can be prepared efficiently and then to slowly deform the initial Hamiltonian \hat{H}_{in} into the final \hat{H}_{out} . A simple example is a linear interpolation scheme

$$\hat{H}(t) = f(t)\hat{H}_{\text{in}} + [1 - f(t)]\hat{H}_{\text{out}}, \quad (3)$$

with some function $f(t)$ satisfying $f(t = 0) = 1$ and $f(t = T) = 0$ where T is the run-time of the algorithm.

If the change from \hat{H}_{in} to \hat{H}_{out} is slow enough, the adiabatic theorem ensures that we indeed end up in the desired final ground state $|\psi_{\text{out}}\rangle$. More precisely, an important condition for adiabatic evolution is that the matrix element of the rate of change $\partial_t \hat{H}$ between two different instantaneous eigen-vectors $\hat{H}(t)|\psi_n(t)\rangle = E_n(t)|\psi_n(t)\rangle$ with instantaneous eigen-energies $E_n(t)$ is small [19, 20]

$$|\langle\psi_n|\partial_t \hat{H}|\psi_m\rangle| \ll (E_n - E_m)^2. \quad (4)$$

Assuming adiabatic evolution and starting in an eigen-vector $|\psi(t=0)\rangle = |\psi_n(t=0)\rangle$ such as the ground state $n = 0$, the time evolved quantum state $|\psi(t)\rangle$ stays close to the instantaneous eigen-vector $|\psi_n(t)\rangle$ up to phase factors containing the dynamical phase $\dot{\varphi}_n^{\text{dyn}}(t) = E_n(t)$ and the geometrical phase $\dot{\varphi}_n^{\text{geo}}(t) = i \langle\psi_n(t)|\partial_t|\psi_n(t)\rangle$.

C. Adiabatic Quantum Search Algorithm

As a simple example for such an adiabatic quantum algorithm, let us consider for a single solution the adiabatic version of Grover's quantum search algorithm [21] as proposed by Roland and Cerf [22]. In the Grover search, the task is to find the solution state $|w\rangle$ as one of the N computational basis states (such as $|w\rangle = |01\dots 10\rangle$) within an unsorted database. Since we obviously do not know the solution $|w\rangle$ beforehand, we choose the superposition state $|s\rangle = \sum_{x=0}^{N-1} |x\rangle / \sqrt{N}$ as the initial state. In an effective spin representation with n spins and $N = 2^n$ basis states and identifying $|\uparrow\rangle = |1\rangle$ and $|\downarrow\rangle = |0\rangle$, this state $|s\rangle = [(|0\rangle + |1\rangle)/\sqrt{2}]^{\otimes n}$ has all spins aligned in x -direction $|s\rangle = |\rightarrow\rangle|\rightarrow\rangle\dots|\rightarrow\rangle$.

A simple realization of the linear interpolation scheme (3) is then

$$\hat{H}(t) = -\Omega[f(t)|s\rangle\langle s| + [1 - f(t)]|w\rangle\langle w|]. \quad (5)$$

In this simple example, the non-trivial quantum evolution is restricted to the subspace spanned by the vectors

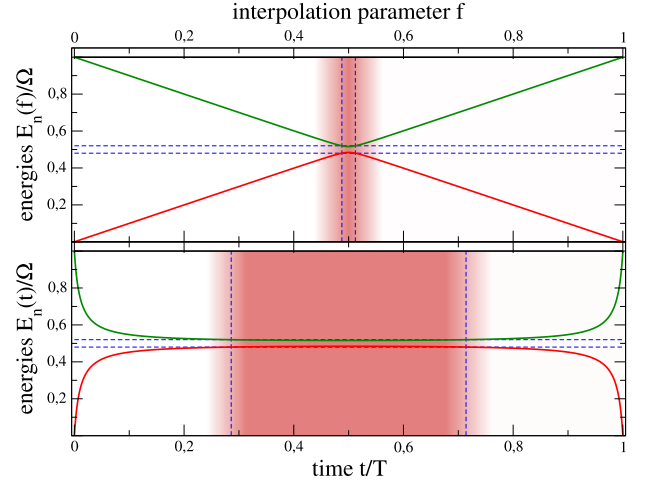


FIG. 1. Top: Shifted spectrum of the Grover Hamiltonian (5) as a function of the interpolation parameter f and $N = 10^3$. For constant-speed interpolation $1 - f(t) = t/T$, little time is spent in the region where the approximations become invalid (shaded region). Bottom: Same spectrum as a function of time and for variable-speed interpolation $\dot{f} \propto \Delta E^2(t)$. The region where typical master equations become invalid is much larger.

$|w\rangle$ and $|s\rangle$ or $|w\rangle$ and $|w_\perp\rangle = |s\rangle - |w\rangle / \sqrt{N} + \mathcal{O}(1/N)$, where we have used the overlap $\langle s|w\rangle = 1/\sqrt{N}$.

Within this subspace, we find an effective Landau-Zener problem

$$\hat{H}(t) \rightarrow -\Omega \begin{pmatrix} 1 - f(t) & f(t)/\sqrt{N} \\ f(t)/\sqrt{N} & f(t) \end{pmatrix} + \mathcal{O}(1/N). \quad (6)$$

As a consequence, we obtain an avoided level crossing at $f(t) = 1/2$ where the overlap $\langle s|w\rangle = 1/\sqrt{N}$ determines the minimum energy gap $\Delta E_{\text{min}} = \Omega/\sqrt{N}$.

Comparison with the adiabatic condition (4) reveals that a constant speed interpolation $\dot{f} = \text{const}$ requires a run-time T of order $T = \mathcal{O}(N)$ in order to satisfy (4) and thus offers no quantum speed-up in comparison to a classical brute-force search. However, interpolations with adaptive speeds such as $\dot{f}(t) \propto [\Delta E(t)]^2$ can yield significantly shorter run-times T of order $T = \mathcal{O}(\sqrt{N})$ which is the usual quadratic quantum speed-up for the Grover search problem [22, 23], see also Fig. 1.

II. PERTURBATION THEORY

One of the motivations for considering adiabatic quantum algorithms was the robustness of the ground state against low-energy noise and decoherence [24, 25]. If we assume that the characteristic frequency ω and energy scales of the environment (such as its temperature) are much smaller than the initial and final energy gap $\Delta E_{\text{max}} = \Omega$ of the Hamiltonian (5), then one would expect that the unavoidable coupling to the environment does not cause problems for preparing the initial

ground state $|s\rangle$ or reading out the final ground state $|w\rangle$. However, since the energy gap becomes extremely small $\Delta E_{\min} = \Omega/\sqrt{N}$ at intermediate times, the impact of the environment may no longer be negligible for the time evolution in between – which is the question we want to study in the following.

To this end, we consider the joint Hilbert space of system plus environment with the total Hamiltonian

$$\hat{H} = \hat{H}_{\text{sys}} + \hat{H}_{\text{env}} + \hat{H}_{\text{int}}, \quad (7)$$

where the system Hamiltonian is given by Eq. (5) and acts on the system Hilbert space (i.e., the qubits), while the intrinsic dynamics of the environment is generated by the environment Hamiltonian \hat{H}_{env} which acts on the environment Hilbert space.

The interaction between system and environment is governed by \hat{H}_{int} which acts on both Hilbert spaces. Neglecting correlated errors of two or more qubits [26–29], we start with the general ansatz

$$\hat{H}_{\text{int}} = g\Omega \sum_{\mu=1}^n \sum_a \hat{\sigma}_{\mu}^a \hat{B}_{\mu}^a. \quad (8)$$

where $\hat{\sigma}_{\mu}^a$ are the usual Pauli spin matrices acting on the qubit μ and \hat{B}_{μ}^a the corresponding bath operators acting on the environment. In order to have dimensionless operators $\hat{\sigma}_{\mu}^a$ and \hat{B}_{μ}^a of order unity, we inserted the energy pre-factor Ω and the small coupling strength $g \ll 1$.

As a first approach, we employ a perturbative expansion in powers of this small coupling strength $g \ll 1$. As usual, in view of the small coupling, we assume that the initial state factorizes (Born approximation)

$$\hat{\rho}(t_{\text{in}}) = \hat{\rho}_{\text{sys}}(t_{\text{in}}) \otimes \hat{\rho}_{\text{env}}^0 = \hat{\rho}_{\text{sys}}^{\text{in}} \otimes \hat{\rho}_{\text{env}}^0, \quad (9)$$

and we employ the interaction picture where the unperturbed dynamics generated by \hat{H}_{sys} and \hat{H}_{env} apply to the operators $\hat{\sigma}_{\mu}^a$ and \hat{B}_{μ}^a , respectively.

A. First Order

Usually, the expectation value of the bath coupling operators is assumed to vanish, but let us also consider the case where $\langle \hat{B}_{\mu}^a \rangle_{\text{env}}^0 \neq 0$. Then, to first order in g , the state of the system evolves as

$$\hat{\rho}_{\text{sys}}^{\text{out}} = \hat{\rho}_{\text{sys}}^{\text{in}} - i \int_{t_{\text{in}}}^{t_{\text{out}}} dt \left[\langle \hat{H}_{\text{int}}(t) \rangle_{\text{env}}^0, \hat{\rho}_{\text{sys}}^{\text{in}} \right] + \mathcal{O}(g^2), \quad (10)$$

where $\langle \hat{H}_{\text{int}}(t) \rangle_{\text{env}}^0 = \text{Tr}_{\text{env}}\{\hat{H}_{\text{int}}(t)\hat{\rho}_{\text{env}}^0\}$ denotes the average over the environment degrees of freedom. Up to this level, we find that the impact of the environment leads to an effective shift $\hat{H}_{\text{sys}} \rightarrow \hat{H}_{\text{sys}}^{\text{eff}} = \hat{H}_{\text{sys}} + \langle \hat{H}_{\text{int}} \rangle_{\text{env}}^0$

of the system Hamiltonian. To study this shift, we may insert the identity operator in the system Hilbert space

$$\begin{aligned} \mathbf{1}_{\text{sys}} &= |w\rangle \langle w| + |w_{\perp}\rangle \langle w_{\perp}| + \sum_{\text{rest}} |\text{rest}\rangle \langle \text{rest}| \\ &= |w\rangle \langle w| + |s\rangle \langle s| - \frac{|w\rangle \langle s| + |s\rangle \langle w|}{\sqrt{N}} \\ &\quad + \sum_{\text{rest}} |\text{rest}\rangle \langle \text{rest}| + \mathcal{O}(1/N), \end{aligned} \quad (11)$$

where the states $|\text{rest}\rangle$ are orthogonal to the sub-space spanned by $|w\rangle$ and $|w_{\perp}\rangle$. The resulting modification of the Landau-Zener Hamiltonian (6) is then determined by the matrix elements of the Pauli spin operators $\hat{\sigma}_{\mu}^a$ multiplied by the expectation values $\langle \hat{B}_{\mu}^a \rangle_{\text{env}}^0$ of the bath operators. Only the diagonal matrix elements $\langle w | \hat{\sigma}_{\mu}^z | w \rangle = \pm 1$ and $\langle s | \hat{\sigma}_{\mu}^x | s \rangle = 1$ are of order unity, the rest is zero or suppressed as $\mathcal{O}(1/\sqrt{N})$, e.g., $\langle w | \hat{\sigma}_{\mu}^z | s \rangle = \pm 1/\sqrt{N}$ or $\langle w | \hat{\sigma}_{\mu}^x | s \rangle = 1/\sqrt{N}$.

As a consequence, the off-diagonal elements of the Landau-Zener Hamiltonian (6) acquire corrections of order $\mathcal{O}(g/\sqrt{N})$ which do not have a significant effect for $g \ll 1$. However, the corrections to the diagonal elements of the Landau-Zener Hamiltonian (6) are much less strongly suppressed and scale with $\mathcal{O}(g)$. Even though they do not change the size of the minimum gap $\Delta E_{\min} = \Omega/\sqrt{N} + \mathcal{O}(g/\sqrt{N})$, they may shift the position of the minimum gap a bit because the environment induced energy shift for the state $|w\rangle$ may well be different from the shift of the other state $|s\rangle$ if $\langle \hat{B}_{\mu}^z \rangle_{\text{env}}^0 \neq \langle \hat{B}_{\mu}^x \rangle_{\text{env}}^0$. If these expectation values are unknown, this could be problematic for executing interpolations with adaptive speeds such as $\dot{f}(t) \propto [\Delta E(t)]^2$, which were required for reaching the quantum speed-up of the Grover search algorithm.

Note that there are also non-zero matrix elements of the Pauli spin operators $\hat{\sigma}_{\mu}^a$ between the states $|w\rangle$ or $|s\rangle$ on the one hand and the remaining states $|\text{rest}\rangle$ on the other hand. As a result, the eigenstates of the shifted system Hamiltonian $\hat{H}_{\text{sys}}^{\text{eff}}$ may also contain a small admixture of those states $|\text{rest}\rangle$ but this does not affect the main properties of the Landau-Zener problem (6).

B. Second Order

As we have observed above, the first-order result (10) amounts to a shift $\hat{H}_{\text{sys}} \rightarrow \hat{H}_{\text{sys}}^{\text{eff}} = \hat{H}_{\text{sys}} + \langle \hat{H}_{\text{int}} \rangle_{\text{env}}^0$ of the system Hamiltonian. If necessary, we may accordingly renormalize the system and interaction Hamiltonians by $\hat{H}_{\text{sys}} \rightarrow \hat{H}_{\text{sys}}^{\text{eff}}$ and $\hat{H}_{\text{int}} \rightarrow \hat{H}_{\text{int}}^{\text{ren}} = \hat{H}_{\text{int}} - \langle \hat{H}_{\text{int}} \rangle_{\text{env}}^0$, after which we have $\langle \hat{H}_{\text{int}}^{\text{ren}} \rangle_{\text{env}}^0 = 0$ and thus the lowest non-trivial contribution is the second order (and the interaction picture for the system operators is then understood

with respect to $\hat{H}_{\text{sys}}^{\text{eff}}$)

$$\begin{aligned} \hat{\rho}_{\text{sys}}^{\text{out}} = & \hat{\rho}_{\text{sys}}^{\text{in}} + g^2 \Omega^2 \sum_{\mu\nu ab} \int_{t_{\text{in}}}^{t_{\text{out}}} dt_1 \int_{t_{\text{in}}}^{t_1} dt_2 \left[\langle \hat{B}_\mu^a(t_1) \hat{B}_\nu^b(t_2) \rangle_{\text{env}}^0 \right. \\ & \times \left(\hat{\sigma}_\mu^a(t_1) \hat{\rho}_{\text{sys}}^{\text{in}} \hat{\sigma}_\nu^b(t_2) - \hat{\sigma}_\mu^a(t_1) \hat{\sigma}_\nu^b(t_2) \hat{\rho}_{\text{sys}}^{\text{in}} \right) + \text{h.c.} \left. \right] \\ & + \mathcal{O}(g^3). \end{aligned} \quad (12)$$

Assuming adiabatic evolution (4) for the system \hat{H}_{sys} , the error probability P_{error} (i.e., the probability for not ending up in the final ground state of \hat{H}_{sys}) is caused by the interaction with the environment and corresponds to the $\mathcal{O}(g^2)$ corrections in Eq. (12). Given a quite general environment, let us now estimate the order of magnitude of the error probability P_{error} .

For a stationary environment, the correlation functions $\langle \hat{B}_\mu^a(t_1) \hat{B}_\nu^b(t_2) \rangle_{\text{env}}^0$ depend on the time difference $t_1 - t_2$ only. Here we assume that they decay on a characteristic time scale τ_{env} and may feature oscillations with typical frequency scales ω_{env} . It is advantageous to distinguish between positive and negative environment frequencies. The former $\omega_{\text{env}} > 0$ mediate excitations of the system while the latter $\omega_{\text{env}} < 0$ correspond to de-excitations. In order to avoid unwanted excitations from the initial and final ground states (as motivated in the Introduction), the positive environment frequencies $\omega_{\text{env}} > 0$ should be much smaller than the initial and final gap $\omega_{\text{env}} \ll \Omega$. For a thermal environment, this means that the environment temperature should also be far below Ω (unless the environment features a large gap in its density of states or spectral coupling density).

Transforming the double time integration in Eq. (12) into the relative $t_- = t_1 - t_2$ and the ‘‘centre-of-mass’’ coordinate $t_+ = (t_1 + t_2)/2$ allows to estimate the scaling: As the interaction picture operators $\hat{\sigma}_\mu^a(t)$ remain normalized, the t_- integration scales with τ_{env} . Additional problems could arise for a highly non-Markovian environment where the spectral function is not well behaved in the infra-red [30–32] such that $\langle \hat{B}_\mu^a(t_1) \hat{B}_\nu^b(t_2) \rangle_{\text{env}}^0$ decays very slowly as a function of $t_1 - t_2$, but we do not consider this case here. Assuming that the total integration time $\Delta t = t_{\text{out}} - t_{\text{in}}$ is much larger than τ_{env} , the remaining time integral over t_+ scales with Δt .

Finally, depending on the spatial range of the correlations in the reservoir, the double sum over all qubits $\sum_{\mu,\nu}$ scales with their number n for short-range correlations or with their number squared n^2 for long-range correlations. Taking the latter case as an upper bound, we may estimate the order of magnitude of the error probability via

$$P_{\text{error}} \leq \mathcal{O}(g^2 \Omega^2 n^2 \tau_{\text{env}} \Delta t). \quad (13)$$

Unfortunately, a small coupling $g \ll 1$ to the environment might not be sufficient to ensure a small error probability. As explained in Sec. IC, the total run-time T scales with $T = \mathcal{O}(\sqrt{N}/\Omega)$ and thus Δt can be very large, i.e., grow exponentially with the number n of

qubits. Since it is probably unrealistic to assume that the coupling g of each qubit to the environment (or the environment correlation time τ_{env}) decreases exponentially if we increase the number n of qubits, i.e., the system size, the above estimate (13) does not allow us to conclude a small error probability.

Let us consider the integrand in Eq. (12) in more detail. Since the coupling $g \ll 1$ is small and $N \gg 1$ is exponentially large, we neglect terms of order $\mathcal{O}(g^2/\sqrt{N})$ in the following. Then assuming adiabatic evolution (4) for the system \hat{H}_{sys} , the unitary system dynamics with $\hat{\sigma}_\mu^a(t) = \hat{U}_{\text{sys}}^\dagger(t) \hat{\sigma}_\mu^a \hat{U}_{\text{sys}}(t)$ can be approximated by [33]

$$\begin{aligned} \hat{U}_{\text{sys}}(t) = & |\psi_0(t)\rangle e^{-i\varphi_0^{\text{dyn}}(t)} \langle s| + |\psi_1(t)\rangle e^{-i\varphi_1^{\text{dyn}}(t)} \langle w| \\ & + \sum_{\text{rest}} |\text{rest}\rangle \langle \text{rest}| + \mathcal{O}\left(\frac{1}{\sqrt{N}}\right). \end{aligned} \quad (14)$$

While $\hat{U}_{\text{sys}}(t)$ does not affect the states $|\text{rest}\rangle$ orthogonal to $|s\rangle$ and $|w\rangle$, it acts as a rotation with a time-dependent angle $\varphi(t)$ within this sub-space. More precisely, up to the dynamical phases $\dot{\varphi}_n^{\text{dyn}}(t) = E_n(t)$, the transformation (14) describes a rotation from the initial ground $|\psi_0(t=0)\rangle = |s\rangle$ and first excited states $|\psi_1(t=0)\rangle = |s_\perp\rangle \approx |w\rangle$ to the instantaneous ground $|\psi_0(t)\rangle$ and first excited state $|\psi_1(t)\rangle$.

Even though the matrix elements of the Pauli spin matrices σ_μ^a between the states $|s\rangle$ and $|w\rangle$ are exponentially suppressed, this is no longer true for the matrix elements between the instantaneous ground and the first excited state, e.g., $\langle \psi_0(t) | \sigma_\mu^z | \psi_1(t) \rangle = \pm \sin[\varphi(t)] \cos[\varphi(t)]$. Since the rotation angle $\varphi(t)$ changes from zero to π when traversing the Landau-Zener transition, the matrix elements mainly contribute in the vicinity of the minimum gap – as one might expect.

In principle, there are also non-zero matrix elements between the instantaneous eigen-vectors $|\psi_0(t)\rangle$ and $|\psi_1(t)\rangle$ on the one hand and the remaining vectors $|\text{rest}\rangle$ on the other hand. However, since the dynamical phases $\dot{\varphi}_0^{\text{dyn}}(t) = E_0(t)$ and $\dot{\varphi}_1^{\text{dyn}}(t) = E_1(t)$ are rapidly oscillating with a frequency $\mathcal{O}(\Omega)$, while the positive environment frequencies $\omega_{\text{env}} \ll \Omega$ are much smaller, the time integrals in Eq. (12) become strongly suppressed for those transitions and thus can be neglected.

For the same reason, transitions from $|\psi_0(t)\rangle$ to $|\psi_1(t)\rangle$ occur predominantly in the vicinity of the minimum gap where the rapid oscillations $\dot{\varphi}_0^{\text{dyn}}(t)$ and $\dot{\varphi}_1^{\text{dyn}}(t)$ almost cancel each other.

III. MASTER EQUATION

The fact that the error probability (13) can become large for long enough time intervals Δt shows that one should not apply perturbation theory (12) to the whole run-time T which is exponentially long $T = \mathcal{O}(\sqrt{N}/\Omega)$. Thus, in order to understand the long-time behavior, a different method is required. One option is a suitable

master equation, see, e.g., [13, 34, 35]. Master equations are usually derived (e.g., in the Nakajima-Zwanzig approach [36, 37]) via a series of approximations, such as Born-Markov and secular approximations. The Born-Markov approximation can be motivated by assuming that the coupling g is small and the environment is large such that all effects on the environment (e.g., correlations between system and environment) are quickly dissipated in the environment, i.e., transported away from the system. As a result, the system always “sees” the same environment, i.e., the environment has no memory, and we can use the ansatz (9) for each time step. In the discussion based on perturbation theory (12) above, this is related to the condition that the environment correlation time τ_{env} is much smaller than Δt .

The secular approximation, on the other hand, can be motivated by assuming that the phase differences between the instantaneous eigen-states of \hat{H}_{sys} are rapidly oscillating such that their time integrals can be neglected. While this assumption is justified for the phase difference between the instantaneous ground state $|\psi_0(t)\rangle$ and the remaining states $|\text{rest}\rangle$, for example, it is not justified for the phase difference between the instantaneous ground state $|\psi_0(t)\rangle$ and the first excited state $|\psi_1(t)\rangle$ which changes extremely slowly in the vicinity of the minimum gap. Thus, the usual secular approximation is problematic for the scenario of interest here [38–41].

A. Coarse Grained Master Equation

In order to overcome this obstacle and to obtain a master equation without the secular approximation, we employ a coarse graining procedure, see also [38, 39, 42, 43]. For simplicity, we only assume coupling terms (8) in σ_μ^z direction for now, other coupling terms will be discussed below.

We split the total evolution time T into many time steps Δt . They should be much larger than the correlation time τ_{env} of the environment and, as discussed above, we apply the Born approximation (9) at each time step. However, these time intervals Δt should still be small enough that we may apply perturbation theory (12) for each time step. This is possible because the coupling g is small. Furthermore, Δt should be much smaller than the total run-time T such that the change of $\hat{U}_{\text{sys}}(t)$ during Δt can be neglected.

In this regime, we may apply basically the same arguments as after Eq. (12) to obtain the form

$$\begin{aligned} \hat{\rho}_{\text{sys}}(t + \Delta t) &\approx \hat{\rho}_{\text{sys}}(t) - i \left[\Delta \hat{H}_{\text{sys}}^{\text{eff}}, \hat{\rho}_{\text{sys}}(t) \right] \\ &+ \Delta t \left[\left(\hat{L} \hat{\rho}_{\text{sys}}(t) \hat{L} - \hat{L}^2 \hat{\rho}_{\text{sys}}(t) \right) + \text{h.c.} \right], \end{aligned} \quad (15)$$

where $\Delta \hat{H}_{\text{sys}}^{\text{eff}} = \mathcal{O}(g^2)$ is a small Lamb-shift type level renormalization term. In the sub-space spanned by $|s\rangle$ and $|w\rangle$, we may use $\hat{U}_{\text{sys}}^\dagger(t) \sigma_\mu^z \hat{U}_{\text{sys}}(t) \approx \hat{U}_{\text{sys}}^\dagger(t) |w\rangle \langle w| \hat{U}_{\text{sys}}(t)$ from Eq. (14), such that we find

the effective Lindblad operator

$$\hat{L}(t) = \sqrt{\Gamma} \hat{U}_{\text{sys}}^\dagger(t) |w\rangle \langle w| \hat{U}_{\text{sys}}(t) = \hat{L}^\dagger(t), \quad (16)$$

which is self-adjoint and whose strength is governed by the effective decay rate, cf. Eq. (13)

$$\Gamma = \mathcal{O}(g^2 \Omega^2 n^2 \tau_{\text{env}}). \quad (17)$$

Transforming from the interaction picture to the Schrödinger picture, we get the same form as in the Lindblad master equation (1)

$$\frac{d\hat{\rho}_{\text{sys}}}{dt} = -i \left[\hat{H}_{\text{sys}}, \hat{\rho} \right] + \hat{L} \hat{\rho} \hat{L}^\dagger - \frac{1}{2} \left\{ \hat{L}^\dagger \hat{L}, \hat{\rho} \right\} \quad (18)$$

in terms of the system Hamiltonian \hat{H}_{sys} while the Lindblad operator \hat{L} is given by $\hat{L} = |w\rangle \sqrt{\Gamma} \langle w|$. This dissipator destroys coherences between the states $|s\rangle$ and $|w\rangle$ and thus slows down transitions in complete analogy to the quantum Zeno effect. As an intuitive picture, the environment is permanently measuring whether the system is in the state $|w\rangle$ or not. Since the effective measurement frequency Γ is not exponentially suppressed (it even increases polynomially with n) while the transition rate governed by \hat{H}_{sys} is exponentially small Ω/\sqrt{N} in the vicinity of the minimum gap, we are in the regime of the quantum Zeno effect for large n .

B. Redfield Equation

As an alternative approach, we may start from the Redfield-I equation [44]. This equation is also based on the Born-Markov approximation, but does not employ the secular approximation. Specifying it to our set-up in Eqs. (7) and (8) in the interaction picture and again assuming coupling terms (8) in σ_μ^z direction only, the Redfield-I equation reads

$$\begin{aligned} \frac{d\hat{\rho}_{\text{sys}}(t)}{dt} &= g^2 \Omega^2 \sum_{\mu\nu} \int_0^t dt' \langle \hat{B}_\mu^z(t) \hat{B}_\nu^z(t') \rangle_{\text{env}}^0 \\ &\times \left(\hat{\sigma}_\nu^z(t') \hat{\rho}_{\text{sys}}(t) \hat{\sigma}_\mu^z(t) - \frac{1}{2} \left\{ \hat{\sigma}_\mu^z(t) \hat{\sigma}_\nu^z(t'), \hat{\rho}_{\text{sys}}(t) \right\} \right. \\ &\quad \left. + \frac{1}{2} \left[\hat{\rho}_{\text{sys}}(t), \hat{\sigma}_\mu^z(t) \hat{\sigma}_\nu^z(t') \right] \right) \\ &+ g^2 \Omega^2 \sum_{\mu\nu} \int_0^t dt' \langle \hat{B}_\mu^z(t') \hat{B}_\nu^z(t) \rangle_{\text{env}}^0 \\ &\times \left(\hat{\sigma}_\nu^z(t) \hat{\rho}_{\text{sys}}(t) \hat{\sigma}_\mu^z(t') - \frac{1}{2} \left\{ \hat{\sigma}_\mu^z(t') \hat{\sigma}_\nu^z(t), \hat{\rho}_{\text{sys}}(t) \right\} \right. \\ &\quad \left. + \frac{1}{2} \left[\hat{\rho}_{\text{sys}}(t), \hat{\sigma}_\mu^z(t') \hat{\sigma}_\nu^z(t) \right] \right). \end{aligned} \quad (19)$$

If we use the same assumption as before, i.e., that the environment correlation time τ_{env} is much shorter than the (exponentially long) time scale on which the system

dynamics changes, we may approximate $\hat{\sigma}_\mu^z(t') \approx \hat{\sigma}_\mu^z(t)$ which allows us to perform the t' integration over the environment correlation function

$$\Gamma = g^2 \Omega^2 \sum_{\mu\nu} \int_0^t dt' \langle \hat{B}_\mu^z(t) \hat{B}_\nu^z(t') \rangle_{\text{env}}^0. \quad (20)$$

As a result, we find the same Lindblad master equation (18) but with a small additional shift of the system Hamiltonian due to the commutator terms $[\hat{\rho}_{\text{sys}}(t), \hat{\sigma}_\mu^z(t) \hat{\sigma}_\nu^z(t)]$ in the third and sixth line of Eq. (19).

Including the σ_μ^x coupling to the environment and using $\hat{U}_{\text{sys}}^\dagger(t) \sigma_\mu^x \hat{U}_{\text{sys}}(t) \approx \hat{U}_{\text{sys}}^\dagger(t) |s\rangle \langle s| \hat{U}_{\text{sys}}(t)$ would give an additional Lindblad operator $|s\rangle \langle s|$ and thus even enhance the quantum Zeno effect, see App. A.

Either way, the quantum Zeno effect would negate the performance of the adiabatic Grover search algorithm since the run-time $T = \mathcal{O}(\sqrt{N})$ describing the usual quadratic quantum speed-up for the Grover search problem in the absence of any environment does not work anymore. As an intuitive picture, the environment permanently measures whether the system is still in the state $|s\rangle$ or already in the state $|w\rangle$ and these permanent measurements inhibit transitions from $|s\rangle$ to $|w\rangle$. From another perspective, these effective measurements destroy the coherences between the states $|s\rangle$ and $|w\rangle$ such that we can no longer add up amplitudes, but we are back to adding up probabilities – such that the main quantum advantage is gone.

In analogy to Sec. I A, one could employ a much longer run-time after which the state approaches the steady state $\hat{\rho} = \mathbf{1}/2$ (in the Landau-Zener sub-space), but this enlarged run-time would scale with $\mathcal{O}(N\Gamma/\Omega^2)$ which means that we lost the quadratic quantum speed-up for the Grover search problem and come back to the usual linear scaling $\mathcal{O}(N)$ of a classical brute-force search.

IV. GENERALIZATION

Having found that the quantum Zeno effect can pose strong restrictions on the performance of the adiabatic quantum search algorithm considered above, one might object that this could be an artifact of the special choice of the Hamiltonian (5) which would be absent for other Hamiltonians. In the following, we show that analogous restrictions should apply to generic Hamiltonians under suitable conditions.

Unfortunately, the generalization to generic Hamiltonians is complicated by the fact that the level structure of general adiabatic quantum algorithms is not fully understood. If we use the same initial projector Hamiltonian as in Eq. (5) but replace the final Hamiltonian by a more realistic version (e.g., bi-linear or tri-linear polynomials of $\hat{\sigma}_\mu^z$ matrices), we can still obtain analytic access to the eigen-states or eigen-energies and it has been shown that the minimum gap does also scale exponentially as

$1/\sqrt{N}$ in this case [45]. Going one step further and also replacing the initial projector Hamiltonian by a paramagnetic Hamiltonian $\propto \sum \sigma_\mu^x$ with the same initial ground state $|s\rangle$, for example, it has been speculated [17] that it might be possible to achieve polynomial scaling of the minimum gap for NP-complete problems [46], but this speculation is under debate. For example, it has been argued [47] that disorder induced localization phenomena should induce a scaling behavior which is even worse than the Grover scaling, i.e., that the minimum gap shrinks faster than $1/\sqrt{N}$ for large N . In this context, it should also be mentioned that the polynomial equivalence between adiabatic and sequential quantum computing has been shown in [48, 49]. This implies that adiabatic quantum algorithms (in the absence of any environment) can achieve an exponential speed-up for factoring – but it does not necessarily imply a similar speed-up for NP-complete problems. At present, it is probably fair to say that this issue has not been fully settled yet.

Nevertheless, we can still draw some conclusions based on general arguments. First of all, adiabatic quantum algorithms are presumably not able to perform non-trivial quantum computations “for free”. Hence, one would expect that the (instantaneous) energy gap between the ground state and the first excited state(s) becomes very small at some point. The external variation, such as $f(t)$ in Eq. (3), must be very slow in order to stay in the adiabatic regime. This point displays similarities to the critical point in a quantum phase transition and a major part of the quantum computation, i.e., a strong change of the quantum (ground) state, is expected to occur in the vicinity of this point [50–53].

In order to support this expectation, let us consider the instantaneous eigen-states $\hat{H}(t) |\psi_n(t)\rangle = E_n(t) |\psi_n(t)\rangle$ where $|\psi_n(t)\rangle$ denotes the parametric time dependence, which should not be confused with the dynamical time dependence of the state $|\psi(t)\rangle$ as a solution of the Schrödinger equation. In the adiabatic regime, they are approximately the same, up to the phases mentioned in Sec. I B. Now let us take the parametric time derivative $|\partial_t \psi_n\rangle$ and split it up into a parallel part $|\partial_t \psi_n\rangle^\parallel \propto |\psi_n\rangle$ (which can be eliminated by a suitable phase transformation) and the remaining perpendicular part $|\partial_t \psi_n\rangle^\perp$ which describes a real rotation in the Hilbert space. Taking the (parametric) time derivative of the equation $\hat{H}(t) |\psi_n(t)\rangle = E_n(t) |\psi_n(t)\rangle$, we find

$$|\partial_t \psi_0\rangle^\perp \Big|^2 \leq \frac{\langle \psi_0 | (\partial_t \hat{H})^2 | \psi_0 \rangle}{\Delta E_0^2}, \quad (21)$$

where ΔE_0 denotes the (instantaneous) energy gap between the ground state and the first excited state(s). As in the Grover search algorithm (5), the major part of the quantum computation, i.e., the strongest change of the quantum (ground) state, is linked to the minimum (or minima) of the energy gap ΔE_0 .

As an intuitive picture, one can visualize $\hat{H}(t)$ via a slowly changing effective potential landscape which

has many local minima (for not-trivial problems to be solved). Starting in the initial ground state, i.e., the global minimum, and deforming the potential landscape, another local minimum may become energetically favourable at some point (the critical point) and the system has to make a (tunneling) transition from the old to the new global minimum. As in the Landau-Zener problem (6), the (tunneling) transition rate determines the minimum gap ΔE_0 at that point.

Now, in the absence of symmetries (see [51, 53]), one would naturally expect that there are probably not more than two competing local minima at that critical point. As a result – and because the minimum gap ΔE_0 is very small – it should be a good approximation to focus on these two states (representing the two competing local minima) for understanding the (tunneling) transition. Indeed, many of the adiabatic quantum algorithms discussed in the literature can be reasonably well approximated by more or less isolated Landau-Zener like avoided level crossings between the two lowest (instantaneous) energy eigen-states (even though there can be many more avoided level crossings at higher lying states).

A. Generalized Landau-Zener Transition

As motivated above, let us consider a general adiabatic quantum algorithm featuring a single isolated Landau-Zener like avoided level crossing which mediates the transition between the two states $|\text{in}\rangle$ and $|\text{out}\rangle$. Here $|\text{in}\rangle$ and $|\text{out}\rangle$ denote the ground states just before and just after the avoided level crossing. They are not necessarily the initial and final ground states, because the ground state could also change away from the avoided level crossing, see Eq. (21).

However, as the transition from $|\text{in}\rangle$ to $|\text{out}\rangle$ is supposed to constitute a major part of the quantum computation, the two states are assumed to be macroscopically different. Here macroscopically different means that $|\text{in}\rangle$ and $|\text{out}\rangle$ disagree for at least a large number $\mathcal{O}(n)$ of qubits. In the Grover search algorithm (5), we have $|\text{in}\rangle = |s\rangle = |\rightarrow\rangle|\rightarrow\rangle\ldots|\rightarrow\rangle$ and $|\text{out}\rangle = |w\rangle = |01\ldots10\rangle = |\downarrow\rangle|\uparrow\rangle\ldots|\uparrow\rangle|\downarrow\rangle$, for example. As a result, the overlap between $|\text{in}\rangle$ and $|\text{out}\rangle$ is exponentially small $\langle\text{in}|\text{out}\rangle = \exp\{-\mathcal{O}(n)\}$, e.g., $\langle s|w\rangle = 1/\sqrt{N}$.

In this case, the matrix elements of the Pauli spin operators $\langle\text{in}|\hat{\sigma}_\mu^a|\text{out}\rangle = \exp\{-\mathcal{O}(n)\}$ are also exponentially small – and the same applies to products of a finite number of Pauli spin operators, such as $\hat{\sigma}_\mu^a\hat{\sigma}_\nu^b$. If we assume a local Hamiltonian, i.e., a sum of polynomially many terms, each acting on a limited number of qubits (e.g., up to two or three), the off-diagonal (transition) matrix element is also exponentially small $\langle\text{in}|\hat{H}|\text{out}\rangle = \exp\{-\mathcal{O}(n)\}$.

The Landau-Zener problem (6) generalizes to

$$\hat{H} \rightarrow \begin{pmatrix} \langle\text{in}|\hat{H}|\text{in}\rangle & \langle\text{in}|\hat{H}|\text{out}\rangle \\ \langle\text{out}|\hat{H}|\text{in}\rangle & \langle\text{out}|\hat{H}|\text{out}\rangle \end{pmatrix}, \quad (22)$$

and thus the minimum gap ΔE_{\min} occurring when the diagonal elements are equal $\langle\text{in}|\hat{H}|\text{in}\rangle = \langle\text{out}|\hat{H}|\text{out}\rangle$ is determined by the off-diagonal matrix element $\Delta E_{\min} = 2|\langle\text{in}|\hat{H}|\text{out}\rangle|$. Consequently, ΔE_{\min} is also exponentially small $\Delta E_{\min} = \exp\{-\mathcal{O}(n)\}$ which means that achieving an exponential speed-up for such an adiabatic quantum algorithm would require violating some of the assumptions above.

Coupling this more general system (22) to an environment as in Eqs. (7) and (8), we may now go through basically the same steps as in Secs. II and III. The unitary system dynamics governing the time evolution in the vicinity of the avoided level crossing can be approximated as in Eq. (14), but with $|s\rangle$ and $|w\rangle$ being replaced by $|\text{in}\rangle$ and $|\text{out}\rangle$, respectively. Deriving the effective Lindblad operators via the coarse grained master equation as in Sec. III A or the Redfield equation in Sec. III B, we find that they are mainly determined by the matrix elements $\langle\text{in}|\hat{\sigma}_\mu^a|\text{in}\rangle$ and $\langle\text{out}|\hat{\sigma}_\mu^a|\text{out}\rangle$, the others are exponentially suppressed.

If we had $\langle\text{in}|\hat{\sigma}_\mu^a|\text{in}\rangle = \langle\text{out}|\hat{\sigma}_\mu^a|\text{out}\rangle$, i.e., if the environment could not distinguish between the two states $|\text{in}\rangle$ and $|\text{out}\rangle$, then the effective Lindblad operators would be effective identity operators (in the subspace spanned by $|\text{in}\rangle$ and $|\text{out}\rangle$) and thus they would become trivial, i.e., the impact of the environment would vanish. However, for macroscopically different states $|\text{in}\rangle$ and $|\text{out}\rangle$, we generically have $\langle\text{in}|\hat{\sigma}_\mu^a|\text{in}\rangle \neq \langle\text{out}|\hat{\sigma}_\mu^a|\text{out}\rangle$ for many matrix elements – which means that the environment can distinguish between the two states $|\text{in}\rangle$ and $|\text{out}\rangle$. As a result, we again find effective Lindblad operators in the form of projectors $|\text{in}\rangle\langle\text{in}|$ and/or $|\text{out}\rangle\langle\text{out}|$.

Since the order of magnitude of the effective decay rate (or measuring frequency) Γ as in Eqs. (17) and (20) is mainly determined by the properties of the environment and its coupling strength g to the system, we find that it is small, but not exponentially suppressed. In contrast, the transition rate of the system itself as determined by $\Delta E_{\min} = \exp\{-\mathcal{O}(n)\}$ is exponentially small, such that we generically have $\Gamma \gg \Delta E_{\min}$ and thus we are again in the regime of the quantum Zeno effect.

V. CONCLUSIONS

The goal of this work is to study the impact of a quite general environment on the performance of adiabatic quantum algorithms, see also [24, 31]. To start with a specific example, we consider the adiabatic version of the Grover search algorithm (in a database with N entries) proposed by Roland and Cerf [22]. Apart from an environment induced shift of the system energies (which may cause problems for adaptive speed interpolations), the main impact of the environment is that it effectively monitors or measures the state of the system with a decoherence rate Γ . Since the minimum gap of the adiabatic quantum algorithm shrinks as $1/\sqrt{N}$ for large N and thus the run-time T grows as \sqrt{N} whereas the properties

of the environment (such as its temperature) and thus the decoherence rate Γ do generically not display such a strong scaling behavior, we find $\Gamma T \gg 1$ for large N . As a result, the quantum Zeno effect inhibits or drastically slows down transitions from the initial state $|s\rangle$ to the desired final state $|w\rangle$.

Note that already a single quasi-particle (photon, phonon or magnon etc.) in the environment whose interaction with only one of the qubits depends on the state of that qubit may induce an effective weak measurement. This problem is even more severe for the usual sequential quantum algorithms, where one single measurement is sufficient to destroy the interference required for the algorithm to work. For adiabatic quantum algorithms, such a single measurement is not necessarily a problem, but frequently repeated measurements can inhibit or slow down the desired quantum evolution. Note that, even for comparable energies (i.e., in the vicinity of the minimum gap), environment-induced transitions between the states $|s\rangle$ and $|w\rangle$ (or other macroscopically different states) are quite unlikely since they imply changing the state of many qubits. In contrast, environment-induced effective (weak) measurements are much more likely since they do not require changing the state of many qubits – they can be performed by acting on one qubit only.

As one would already expect from the above arguments, analogous conclusions apply to more general adiabatic quantum algorithms under certain assumptions (such as isolated Landau-Zener type avoided level crossings). Thus, while we did not prove that all adiabatic quantum algorithms suffer from this problem, our results strongly suggest to carefully consider the impact of an environment when trying to implement adiabatic quantum algorithms with many qubits (or other degrees of freedom).

VI. OUTLOOK

For the usual sequential quantum algorithms, the problem of decoherence as briefly sketched above has stimulated a substantial amount of work devoted to the development of error correcting codes such as the Shor code [26–28]. In the case of adiabatic quantum algorithms, it is hard to see how such active error correcting codes could be applied directly, but one could envision other, more indirect, methods. One prominent example is the spin-echo technique where the overall phase of the system is frequently changed (e.g., reversed) without affecting the phase of the environment, such that the amplitudes of the interaction between system and environment average out to zero if this phase-flip frequency is large enough, i.e., larger than effective environment frequency scales (such as the environment temperature). Of course, by applying this idea, one must be careful to ensure that the repeated phase change of the system does not affect the adiabaticity of the internal system dynamics. Another option would be to encode the two states

$|s\rangle$ and $|w\rangle$ within a decoherence-free subspace such that the environment cannot distinguish between them (see also Sec. IV). Alternatively, one might consider monitoring the environment and using feedback control similar to quantum erasure schemes [14]. Furthermore, one could consider replacing the Landau-Zener like (tunneling) transition between macroscopically different quantum states such as $|s\rangle$ and $|w\rangle$ (which is very similar to a first-order phase transition) by a more gradual change of the state vectors from $|s\rangle$ to $|w\rangle$, e.g., similarly to a second-order transition [51, 53]. This may even lead to an enlarged minimum gap and thus a reduced run-time T . In addition, such a gradual change should also alleviate the quantum Zeno mechanism sketched above. As a related point, the quantum Zeno effect considered here (and actually in most other scenarios) is applied to the (tunneling) transition between the two isolated states $|s\rangle$ and $|w\rangle$. If instead a continuum of states is involved, the character of the quantum Zeno effect changes and the required measurement frequency is typically much higher [10]. In this case, the inverse decoherence rate $1/\Gamma$ should not be compared to the run-time T but to the spreading time in the continuum, which can be much shorter.

Apart from solving classical problems such as searching a database or factoring numbers, qubit architectures can also be used as quantum simulators for physical systems [54]. For example, false vacuum decay has recently been simulated using several thousands of qubits [55]. There are several similarities to the case considered here (such as the analogy to first-order transitions), but also some important differences. For example, false vacuum decay does typically not occur as a global transition between two states such as $|s\rangle$ and $|w\rangle$. Instead, it generally starts with a local nucleation seed (e.g., a few qubits are in the “correct” vacuum state while all the other are still in the false vacuum state) which then spreads out. Still, it would be interesting to study the impact of the environment, e.g., regarding the quantum Zeno effect.

In this context, quantum annealers or quantum annealing have also been discussed. Not that the term “quantum annealing” is not uniquely defined and can refer to different scenarios, ranging from quantum inspired classical algorithms to quantum algorithms which are also based on the adiabatic passage in a Landau-Zener type avoided level crossing. For the latter, the quantum Zeno effect induced by the environment should also be taken into account, as explained in the previous section.

ACKNOWLEDGMENTS

Funded by the Deutsche Forschungsgemeinschaft (DFG, German Research Foundation) through the Collaborative Research Center SFB 1242 “Nonequilibrium dynamics of condensed matter in the time domain” (Project-ID 278162697). R.S. has benefited from the activities of COST Action CA23115: Relativistic Quantum

-
- [1] B. Misra and E. C. G. Sudarshan. The Zeno's paradox in quantum theory. *Journal of Mathematical Physics*, 18(4):756–763, 04 1977.
- [2] Wayne M. Itano, D. J. Heinzen, J. J. Bollinger, and D. J. Wineland. Quantum Zeno effect. *Phys. Rev. A*, 41:2295–2300, Mar 1990.
- [3] G. Hackenbroich, B. Rosenow, and H. A. Weidenmüller. Quantum Zeno effect and parametric resonance in mesoscopic physics. *Phys. Rev. Lett.*, 81:5896–5899, Dec 1998.
- [4] M. C. Fischer, B. Gutiérrez-Medina, and M. G. Raizen. Observation of the quantum Zeno and anti-Zeno effects in an unstable system. *Phys. Rev. Lett.*, 87:040402, Jul 2001.
- [5] S. A. Gurvitz, L. Fedichkin, D. Mozyrsky, and G. P. Berman. Relaxation and the Zeno effect in qubit measurements. *Phys. Rev. Lett.*, 91:066801, Aug 2003.
- [6] Erik W. Streed, Jongchul Mun, Micah Boyd, Gretchen K. Campbell, Patrick Medley, Wolfgang Ketterle, and David E. Pritchard. Continuous and pulsed quantum Zeno effect. *Phys. Rev. Lett.*, 97:260402, Dec 2006.
- [7] J. Bernu, S. Deléglise, C. Sayrin, S. Kuhr, I. Dotsenko, M. Brune, J. M. Raimond, and S. Haroche. Freezing coherent field growth in a cavity by the quantum zeno effect. *Phys. Rev. Lett.*, 101:180402, Oct 2008.
- [8] D H Slichter, C Müller, R Vijay, S J Weber, A Blais, and I Siddiqi. Quantum Zeno effect in the strong measurement regime of circuit quantum electrodynamics. *New Journal of Physics*, 18(5):053031, may 2016.
- [9] E. Blumenthal, C. Mor, A. A. Diringer, L. S. Martin, P. Lewalle, D. Burgarth, K. B. Whaley, and S. Hacohe-Gourgy. Demonstration of universal control between non-interacting qubits using the quantum Zeno effect. *npj Quantum Information*, 8:88, 2022.
- [10] N. Ahmadi-iaz, M. Geller, J. König, P. Kratzer, A. Lorke, G. Schaller, and R. Schützhold. Quantum Zeno manipulation of quantum dots. *Phys. Rev. Research*, 4:L032045, Sep 2022.
- [11] Yakir Aharonov, Eliahu Cohen, and Avshalom C. Elitzur. Foundations and applications of weak quantum measurements. *Phys. Rev. A*, 89:052105, May 2014.
- [12] R. E. Kastner. Demystifying weak measurements. *Foundations of Physics*, 47(5):697–707, 2017.
- [13] Heinz-Peter Breuer and Francesco Petruccione. *The Theory of Open Quantum Systems*. Oxford University Press, 01 2007.
- [14] H. M. Wiseman and G. J. Milburn. *Quantum Measurement and Control*. Cambridge University Press, Cambridge, 2010.
- [15] Michael A. Nielsen and Isaac L. Chuang. *Quantum Computation and Quantum Information*. Cambridge University Press, Cambridge, 2000.
- [16] W. van Dam, M. Mosca, and U. Vazirani. How powerful is adiabatic quantum computation? In *Proceedings 42nd IEEE Symposium on Foundations of Computer Science*, pages 279–287, 2001.
- [17] Edward Farhi, Jeffrey Goldstone, Sam Gutmann, Joshua Lapan, Andrew Lundgren, and Daniel Preda. A quantum adiabatic evolution algorithm applied to random instances of an NP-complete problem. *Science*, 292(5516):472–475, 2001.
- [18] Tameem Albash and Daniel A. Lidar. Adiabatic quantum computation. *Rev. Mod. Phys.*, 90:015002, Jan 2018.
- [19] M. S. Sarandy, L.-A. Wu, and D. A. Lidar. Consistency of the adiabatic theorem. *Quantum Information Processing*, 3(6):331–349, 2004.
- [20] Sabine Jansen, Mary-Beth Ruskai, and Ruedi Seiler. Bounds for the adiabatic approximation with applications to quantum computation. *Journal of Mathematical Physics*, 48(10):102111, 10 2007.
- [21] Lov K. Grover. Quantum mechanics helps in searching for a needle in a haystack. *Phys. Rev. Lett.*, 79:325–328, Jul 1997.
- [22] Jérémie Roland and Nicolas J. Cerf. Quantum search by local adiabatic evolution. *Physical Review A*, 65:042308, Mar 2002.
- [23] Gernot Schaller, Sarah Mostame, and Ralf Schützhold. General error estimate for adiabatic quantum computing. *Physical Review A*, 73:062307, 2006.
- [24] Andrew M. Childs, Edward Farhi, and John Preskill. Robustness of adiabatic quantum computation. *Phys. Rev. A*, 65:012322, Dec 2001.
- [25] Johan Åberg, David Kult, and Erik Sjöqvist. Robustness of the adiabatic quantum search. *Phys. Rev. A*, 71:060312, Jun 2005.
- [26] Peter W. Shor. Scheme for reducing decoherence in quantum computer memory. *Physical Review A*, 52:R2493–R2496, Oct 1995.
- [27] Andrew Steane. Multiple-particle interference and quantum error correction. *Proceedings of the Royal Society of London. Series A: Mathematical, Physical and Engineering Sciences*, 452(1954):2551–2577, 1996.
- [28] Raymond Laflamme, Cesar Miquel, Juan Pablo Paz, and Wojciech Hubert Zurek. Perfect quantum error correcting code. *Phys. Rev. Lett.*, 77:198–201, Jul 1996.
- [29] Austin G. Fowler and John M. Martinis. Quantifying the effects of local many-qubit errors and nonlocal two-qubit errors on the surface code. *Phys. Rev. A*, 89:032316, Mar 2014.
- [30] Peter Hänggi. Correlation functions and master equations of generalized (non-Markovian) Langevin equations. *Zeitschrift für Physik B Condensed Matter*, 31(4):407–416, 1978.
- [31] M. Tiersch and R. Schützhold. Non-Markovian decoherence in the adiabatic quantum search algorithm. *Physical Review A*, 75:062313, 2007.
- [32] Jinshuang Jin, Christian Karlewski, and Michael Marthaler. Non-Markovian correlation functions for open quantum systems. *New Journal of Physics*, 18(8):083038, aug 2016.
- [33] Note that the geometrical phase vanishes for the adiabatic Grover search.
- [34] U. Weiss. *Quantum Dissipative Systems*, volume 2 of *Series of Modern Condensed Matter Physics*. World Scientific, Singapore, 1993.
- [35] M. Schlosshauer. *Decoherence and the Quantum-To-Classical Transition*. Springer, Berlin, 2007.

- [36] Sadao Nakajima. On Quantum Theory of Transport Phenomena: Steady Diffusion. *Progress of Theoretical Physics*, 20(6):948–959, 12 1958.
- [37] Robert Zwanzig. Ensemble method in the theory of irreversibility. *The Journal of Chemical Physics*, 33(5):1338–1341, 1960.
- [38] G. Schaller and T. Brandes. Preservation of positivity by dynamical coarse-graining. *Physical Review A*, 78:022106, 2008.
- [39] Christian Majenz, Tameem Albash, Heinz-Peter Breuer, and Daniel A. Lidar. Coarse graining can beat the rotating-wave approximation in quantum markovian master equations. *Phys. Rev. A*, 88:012103, Jul 2013.
- [40] H. Mäkelä and M. Möttönen. Effects of the rotating-wave and secular approximations on non-Markovianity. *Phys. Rev. A*, 88:052111, Nov 2013.
- [41] Felipe Matus, Jan Štřeleček, Pavel Stránský, and Pavel Cejnar. Search for optimal driving in finite quantum systems with precursors of criticality. *Phys. Rev. A*, 107:012216, Jan 2023.
- [42] F. Benatti, R. Floreanini, and U. Marzolino. Environment-induced entanglement in a refined weak-coupling limit. *epl*, 88(2), 2009.
- [43] Ángel Rivas. Refined weak-coupling limit: Coherence, entanglement, and non-Markovianity. *Physical Review A*, 95:042104, Apr 2017.
- [44] A. G. Redfield. *Advances in Magnetic and Optical Resonance*, chapter The Theory of Relaxation Processes, pages 1–32. Advances in Magnetic and Optical Resonance. Academic Press, New York, 1965.
- [45] Marko Znidaric and Martin Horvat. Exponential complexity of an adiabatic algorithm for an NP-complete problem. *Physical Review A*, 73:022329, 2006.
- [46] Andrew Lucas. Ising formulations of many NP problems. *Frontiers in Physics*, 2:5, 2014.
- [47] Boris Altshuler, Hari Krovi, and Jérémie Roland. Anderson localization makes adiabatic quantum optimization fail. *Proceedings of the National Academy of Sciences*, 107(28):12446–12450, 2010.
- [48] Dorit Aharonov, Wim van Dam, Julia Kempe, Zeph Landau, Seth Lloyd, and Oded Regev. Adiabatic quantum computation is equivalent to standard quantum computation. *SIAM Journal on Computing*, 37(1):166–194, 2007.
- [49] Ari Mizel, Daniel A. Lidar, and Morgan Mitchell. Simple proof of equivalence between adiabatic quantum computation and the circuit model. *Phys. Rev. Lett.*, 99:070502, Aug 2007.
- [50] José Ignacio Latorre and Román Orús. Adiabatic quantum computation and quantum phase transitions. *Phys. Rev. A*, 69:062302, Jun 2004.
- [51] R. Schützhold and G. Schaller. Adiabatic quantum algorithms as quantum phase transitions: First versus second order. *Physical Review A*, 74:060304(R), 2006.
- [52] M. H. S. Amin and V. Choi. First-order quantum phase transition in adiabatic quantum computation. *Phys. Rev. A*, 80:062326, Dec 2009.
- [53] G. Schaller and R. Schützhold. The role of symmetries in adiabatic quantum algorithms. *Quantum Information and Computation*, 10:0109–0140, 2010.
- [54] J. D. Biamonte, V. Bergholm, J. D. Whitfield, J. Fitzsimons, and A. Aspuru-Guzik. Adiabatic quantum simulators. *AIP Advances*, 1(2):022126, 05 2011.
- [55] Jaka Vodeb, Jean-Yves Desaulles, Andrew Hallam, Andrea Rava, Gregor Humar, Dennis Willsch, Fengping Jin, Madita Willsch, Kristel Michielsen, and Zlatko Papić. Stirring the false vacuum via interacting quantized bubbles on a 5,564-qubit quantum annealer. *Nature Physics*, 21(3):386–392, 2025.
- [56] A.O Caldeira and A.J Leggett. Quantum tunnelling in a dissipative system. *Annals of Physics*, 149(2):374–456, 1983.
- [57] Tameem Albash, Sergio Boixo, Daniel A Lidar, and Paolo Zanardi. Quantum adiabatic Markovian master equations. *New Journal of Physics*, 14(12):123016, dec 2012.
- [58] Gabriel T. Landi, Dario Poletti, and Gernot Schaller. Nonequilibrium boundary-driven quantum systems: Models, methods, and properties. *Rev. Mod. Phys.*, 94:045006, Dec 2022.
- [59] Gernot Schaller, Javier Cerrillo, Georg Engelhardt, and Philipp Strasberg. Electronic Maxwell demon in the coherent strong-coupling regime. *Phys. Rev. B*, 97:195104, May 2018.
- [60] P. F. Palmer. The singular coupling and weak coupling limits. *Journal of Mathematical Physics*, 18(3):527–529, 1977.
- [61] M. G. Schultz and F. von Oppen. Quantum transport through nanostructures in the singular-coupling limit. *Physical Review B*, 80:033302, 2009.
- [62] Anton Trushechkin. Unified Gorini-Kossakowski-Lindblad-Sudarshan quantum master equation beyond the secular approximation. *Phys. Rev. A*, 103:062226, Jun 2021.

Appendix A: Freezing via Lindblad dissipation

We can write Eq. (2) also as $\frac{d}{dt}\langle\hat{\sigma}\rangle = M\langle\hat{\sigma}\rangle$ with matrix

$$M = \begin{pmatrix} -2\Gamma & 0 & 2\Omega \\ 0 & -2\Gamma & 0 \\ -2\Omega & 0 & 0 \end{pmatrix}, \quad (\text{A1})$$

and the eigenvalues of this matrix $\lambda_0 = -2\Gamma$ and $\lambda_{\pm} = -\Gamma \pm \sqrt{\Gamma^2 - 4\Omega^2}$ then support the discussion in the main text in the respective limits.

When we consider two hermitian Lindblad operators $\hat{L}_1 = \sqrt{\Gamma_1} |\uparrow\rangle\langle\uparrow|$ or $\hat{L}_2 = \sqrt{\Gamma_2} |\downarrow\rangle\langle\downarrow|$ instead, this changes into

$$M = \begin{pmatrix} -(\Gamma_1 + \Gamma_2)/2 & 0 & 2\Omega \\ 0 & -(\Gamma_1 + \Gamma_2)/2 & 0 \\ -2\Omega & 0 & 0 \end{pmatrix}, \quad (\text{A2})$$

with analogous conclusions on the eigenvalues $\lambda_0 = -(\Gamma_1 + \Gamma_2)/2$ and $\lambda_{\pm} = -(\Gamma_1 + \Gamma_2) \pm \sqrt{(\Gamma_1 + \Gamma_2)^2 - 64\Omega^2}/4$.

Comparing (A1) and (A2) we see that a σ^z Lindblad operator is more effective in dampening than e.g. a $|\uparrow\rangle\langle\uparrow|$ Lindblad operator as it acts on both states.

In contrast, a non-hermitian Lindblad operator cannot be used to stabilize a state. Considering for example the

relaxation operator $\hat{L} = \sqrt{\sigma} |\downarrow\rangle \langle \uparrow|$, we arrive at

$$M = \begin{pmatrix} -\sigma/2 & 0 & 2\Omega \\ 0 & -\sigma/2 & 0 \\ -2\Omega & 0 & -\sigma \end{pmatrix}, \quad (\text{A3})$$

which has eigenvalues $\lambda_0 = -\sigma/2$ and $\lambda_{\pm} = (-3\sigma \pm \sqrt{\sigma^2 - 64\Omega^2})/4$ which all maintain negative real parts in all regimes.

More generally, hermitian Lindblad operators can be associated with the Zeno effect. In the eigenbasis of the measured observable, the net effect of repeated measurements is the erasure of coherences, which always increases the von-Neumann entropy of the measured system. When we write (1) with hermitian Lindblad operators $\hat{L} = \hat{L}^\dagger$ (multiple Lindblad operators work analogously) one can see that such dephasing dissipators also never decrease the von-Neumann entropy of the system:

$$\begin{aligned} \frac{d}{dt} S &= -\text{Tr} \left\{ \frac{d\hat{\rho}}{dt} \ln \hat{\rho} \right\} = -\text{Tr} \left\{ (\hat{L}\hat{\rho}\hat{L} - \hat{L}^2\hat{\rho}) \ln \hat{\rho} \right\} \\ &= \sum_{ab} L_{ab} L_{ba} \rho_a \ln \left(\frac{\rho_a L_{ab} L_{ba}}{\rho_b L_{ab} L_{ba}} \right) \geq 0, \end{aligned} \quad (\text{A4})$$

where in the first equality sign we have used that the term with the time derivative acting on the $\ln \hat{\rho}$ term does not contribute under the trace, in the second equality we exploited the invariance of the trace under cyclic permutations, and in the third equality we have evaluated the trace in the eigenbasis of the density matrix $\hat{\rho} = \sum_a \rho_a |a\rangle \langle a|$ with $L_{ab} = \langle a| \hat{L} |b\rangle$ and inserted the identity in the logarithm, to eventually use the logarithmic sum inequality in the last step.

When additionally the Lindblad operators do not commute with the Hamiltonian, e.g. $\hat{L} = \Gamma \hat{O}$ with $[\hat{H}, \hat{O}] \neq 0$, we can see an analogous slowing down of relaxation by dissipation: Representing the density matrix $\hat{\rho} = \sum_{\ell m} \rho_{\ell m} |\ell\rangle \langle m|$ now in the eigenbasis of the Lindblad operator defined via $\hat{O} |\ell\rangle = \lambda_\ell |\ell\rangle$, its matrix elements obey

$$\begin{aligned} \dot{\rho}_{\ell m} &= -i \sum_n \rho_{nm} \langle \ell | \hat{H} | n \rangle + i \sum_n \rho_{\ell n} \langle n | \hat{H} | m \rangle \\ &\quad - \frac{\Gamma}{2} (\lambda_\ell - \lambda_m)^2 \rho_{\ell m}. \end{aligned} \quad (\text{A5})$$

This implies that the diagonal elements just follow the evolution of the off-diagonals $\dot{\rho}_{\ell\ell} = -i \sum_{n \neq \ell} \langle \ell | \hat{H} | n \rangle \rho_{n\ell} + i \sum_{n \neq \ell} \langle n | \hat{H} | \ell \rangle \rho_{\ell n}$, whereas the off-diagonal matrix elements will for large Γ rapidly approach a flow equilibrium value (denoted by overbars) that is given by the diagonals

$$\frac{\Gamma}{2} (\lambda_\ell - \lambda_n)^2 \bar{\rho}_{\ell n} \approx i \langle \ell | \hat{H} | n \rangle (\rho_{\ell\ell} - \rho_{nn}). \quad (\text{A6})$$

By eliminating the off-diagonal matrix elements in the

equation for the diagonals, we obtain a rate equation

$$\dot{\rho}_{\ell\ell} \approx \sum_{n \neq \ell} \frac{4 |\langle \ell | \hat{H} | n \rangle|^2}{\Gamma (\lambda_\ell - \lambda_n)^2} \rho_{nn} - \left[\sum_{n \neq \ell} \frac{4 |\langle \ell | \hat{H} | n \rangle|^2}{\Gamma (\lambda_\ell - \lambda_n)^2} \right] \rho_{\ell\ell}, \quad (\text{A7})$$

which evolves slowly – with rates of order $\mathcal{O}\{\hat{H}^2/\Gamma\}$ – towards a complete statistical mixture. The stronger the dissipation in comparison to the system Hamiltonian, the slower is this secondary evolution, and as we have expressed the problem in the eigenbasis of \hat{L} , its eigenstates are precisely the ones that are stabilized.

While Lindblad dynamics is typically observed in weak-coupling scenarios, we stress that the Zeno inhibition may be observed when H_S is small in comparison to Γ . Furthermore, a frozen evolution due to strong dissipation can also be observed beyond Lindblad master equation scenarios as we show for a particular example in App. B

Appendix B: Freezing via strong dissipation

To observe the Zeno effect beyond a weak-coupling scenario, we may consider a Caldeira-Leggett [56] type model of a frequency-driven oscillator with position \hat{x} and momentum \hat{p} that is coupled to a reservoir of oscillators

$$\begin{aligned} H(t) &= \frac{\hat{p}^2}{2m} + \frac{1}{2} m \Omega^2(t) \hat{x}^2 \\ &\quad + \sum_k \omega_k \left(\hat{b}_k^\dagger + \frac{h_k}{\omega_k} \hat{x} \right) \left(\hat{b}_k + \frac{h_k^*}{\omega_k} \hat{x} \right). \end{aligned} \quad (\text{B1})$$

The operators then obey the Heisenberg equations of motion (we omit the time-dependence of the frequency below for brevity)

$$\begin{aligned} \frac{d}{dt} \hat{x}(t) &= \frac{\hat{p}(t)}{m}, \\ \frac{d}{dt} \hat{p}(t) &= - \left(m \Omega^2 + 2 \sum_k \frac{|h_k|^2}{\omega_k} \right) \hat{x}(t) \\ &\quad - \sum_k \left(h_k \hat{b}_k(t) + h_k^* \hat{b}_k^\dagger(t) \right), \\ \frac{d}{dt} \hat{b}_k(t) &= -i \omega_k \hat{b}_k(t) - i h_k^* \hat{x}(t). \end{aligned} \quad (\text{B2})$$

In these, we may eliminate the reservoir modes and arrive at coupled equations for $\hat{x}(t)$ and $\hat{p}(t)$ only. Introducing the spectral function of the reservoir $\Gamma(\omega) = 2\pi \sum_k |h_k|^2 \delta(\omega - \omega_k)$ and taking expectation values with the assumption of an initial product state with a reservoir state with $\langle \hat{b}_k \rangle = 0$ (e.g. a thermal one), we further obtain an integro-differential (non-Markovian) equation

for position and momentum

$$\begin{aligned} \frac{d}{dt}\langle\hat{p}\rangle_t &= -\left(m\Omega^2 + \frac{1}{\pi}\int_0^\infty \frac{\Gamma(\omega)}{\omega}d\omega\right)\langle\hat{x}\rangle_t \\ &\quad + \int_0^t dt' \frac{1}{\pi}\int_0^\infty d\omega \Gamma(\omega) \sin(\omega(t-t'))\langle\hat{x}\rangle_{t'}, \\ \frac{d}{dt}\langle\hat{x}\rangle_t &= \frac{\langle\hat{p}\rangle_t}{m}. \end{aligned} \quad (\text{B3})$$

Now, particularly for the spectral function

$$\Gamma(\omega) = \Gamma_0 \frac{\omega\omega_c}{\omega^2 + \omega_c^2}, \quad (\text{B4})$$

we observe that the memory kernel has a simple exponential dependence

$$\begin{aligned} \frac{d}{dt}\langle\hat{p}\rangle_t &= -\left(m\Omega^2 + \frac{\Gamma_0}{2}\right)\langle\hat{x}\rangle_t + \int_0^t dt' \frac{\Gamma_0\omega_c}{2} e^{-\omega_c(t-t')}\langle\hat{x}\rangle_{t'}, \\ \frac{d}{dt}\langle\hat{x}\rangle_t &= \frac{\langle\hat{p}\rangle_t}{m}. \end{aligned} \quad (\text{B5})$$

This form has the tremendous advantage that also for finite ω_c we may alternatively solve the time-local enlarged system

$$\begin{aligned} \frac{d}{dt}\langle\hat{p}\rangle_t &= -\left(m\Omega^2 + \frac{\Gamma_0}{2}\right)\langle\hat{x}\rangle_t + B_t, \\ \frac{d}{dt}\langle\hat{x}\rangle_t &= \langle\hat{p}\rangle_t/m, \\ \frac{d}{dt}B_t &= \frac{\Gamma_0\omega_c}{2}\langle\hat{x}\rangle_t - \omega_c B_t \end{aligned} \quad (\text{B6})$$

with the initial condition $B_0 = 0$.

We can introduce the dimensionless variables $\tilde{x} = \sqrt{2m\Omega}\langle\hat{x}\rangle_t$, $\tilde{p} = \sqrt{2/(m\Omega)}\langle\hat{p}\rangle_t$, $\tilde{B} = \sqrt{2/(m\Omega^3)}B_t$ and the dimensionless time $\tau = \Omega t$, such that the vector $\mathbf{r} = (\tilde{x}, \tilde{p}, \tilde{B})$ obeys $\left(1 + \frac{\tau\tilde{\Omega}}{2}\right) \frac{d}{d\tau}\mathbf{r}(\tau) = M\mathbf{r}(\tau)$ with the coefficient matrix

$$M = \begin{pmatrix} 0 & 1 & 0 \\ -(1+\alpha) & 0 & 1 \\ \alpha\beta & 0 & -\beta \end{pmatrix}, \quad (\text{B7})$$

where $\alpha = \frac{\Gamma_0}{2m\Omega^2} \geq 0$ denotes a dimensionless damping strength and $\beta = \frac{\omega_c}{\Omega} \geq 0$ a dimensionless reservoir memory scale. Thus, the time-local evolution is governed by the τ -dependent eigenvalues of M , and the strong-coupling regime can be reached by small Ω . The eigenvalues of M all have a non-positive real part and can be expressed in terms of radicals. Furthermore, beyond a certain damping strength $\alpha > 8$ and for $\frac{\sqrt{\alpha^2 + 20\alpha - 8} - \sqrt{\alpha(\alpha-8)^{3/2}}}{2^{3/2}} < \beta < \frac{\sqrt{\alpha^2 + 20\alpha - 8} + \sqrt{\alpha(\alpha-8)^{3/2}}}{2^{3/2}}$ all eigenvalues are just real negative. When $\beta = 3\sqrt{\frac{\alpha-2}{2}}$ and $\alpha \geq 8$, the eigenvalues read

$$\begin{aligned} \lambda_1 &= \frac{\sqrt{\alpha-8} - \sqrt{\alpha-2}}{\sqrt{2}}, & \lambda_2 &= -\frac{\sqrt{\alpha-2}}{\sqrt{2}}, \\ \lambda_3 &= -\frac{\sqrt{\alpha-8} + \sqrt{\alpha-2}}{\sqrt{2}}, \end{aligned} \quad (\text{B8})$$

from which we see that the first tends to zero $\lim_{\alpha \rightarrow \infty} \lambda_1 = -3/\sqrt{2\alpha}$ (Zeno stabilization). The corresponding right eigenvector is given by

$$v_1 = \begin{pmatrix} 1 \\ \lambda_1 \\ \alpha + 1 + \lambda_1^2 \end{pmatrix} \frac{1}{\sqrt{1 + \lambda_1^2 + (\alpha + 1 + \lambda_1^2)^2}}, \quad (\text{B9})$$

which shows that states with a negligible momentum component will be stabilized for large α (small $|\lambda_1|$). Classically, this Zeno inhibition just corresponds to the overdamped limit, where momentum first settles rapidly to a flow equilibrium value and then position relaxes extremely slowly.

Appendix C: Adiabatic master equation

In the adiabatic master equation of Lindblad form, one assumes strictly adiabatic time evolution (4) and performs the Born- and Markov approximations as usual. This results in a time-dependent Redfield equation that is not of Lindblad form and thereby only preserves trace and hermiticity but not positivity of the system density matrix. To obtain a Lindblad form in general, a secular approximation is already required for undriven systems. Analogously, for adiabatically driven systems, a generalized secular approximation can be performed that eventually leads to a Lindblad master equation, see Eqns. (54) in Ref. [57]. Technically, one could obtain the adiabatic master equation also from the time-independent problem (see e.g. Eq. (32) from Ref. [58]) by inserting the time-dependencies of eigenvalues and eigenstates *a posteriori*. Thus, the favorable properties of the Born-Markov-secular master equation also transfer to the adiabatic version and one obtains a decoupled evolution of populations and coherences for non-degenerate systems. The populations then follow a Pauli-type rate equation as e.g. given by Eq. (36) of Ref. [58], but where the time-dependent rates are evaluated at the instantaneous energies. This then also implies that a Zeno blockade cannot be observed in the adiabatic master equation as the ground state will always be favored when the temperature is not much larger than the minimum gap. Consistently, the Zeno blockades observed earlier by some of us [59] have been obtained using master equations that do not decouple populations and coherences in the energy eigenbasis.

Thus, we object that the generalized secular approximation will fail when the driving protocol leads to small energy gaps (e.g. the shaded regions in Fig. 1) as is unfortunately the case for most adiabatic algorithms. Consequently, the results from the associated adiabatic master equation (and resulting Pauli rate equation) should only be trusted in regimes where the gap remains large (white regions in Fig. 1).

Appendix D: Singular coupling master equation

When the gap is negligible in comparison to the system-reservoir coupling strength (deep within the shaded regions in Fig. 1), one can also derive a master equation by treating both $\hat{H}_{\text{sys}}(t)$ and \hat{H}_{int} as perturbation. This is then possible as in the relevant near-degenerate subspace the system Hamiltonian (up to a trivial shift) only opens a small gap and is thus small in comparison to the interaction. This scenario is analogous to the singular coupling limit [60]. More explicitly, starting from $\hat{H}_{\text{int}} = g \sum_{\alpha} \hat{A}_{\alpha} \otimes \hat{B}_{\alpha}$ (the system operators \hat{A}_{α} and reservoir operators \hat{B}_{α} can always be chosen individually hermitian), the interaction picture Hamiltonian becomes

$$\begin{aligned}\hat{H}(t) &= \hat{H}_{\text{sys}}(t) + g \sum_{\alpha} \hat{A}_{\alpha} \otimes \hat{B}_{\alpha}(t), \\ \hat{B}_{\alpha}(t) &= e^{+i\hat{H}_{\text{env}}t} \hat{B}_{\alpha} e^{-i\hat{H}_{\text{env}}t},\end{aligned}\tag{D1}$$

and by iteratively solving the von-Neumann equation neglecting terms of $\mathcal{O}\{H_{\text{int}}^3\}$ and $\mathcal{O}\{H_{\text{int}}H_{\text{sys}}(t)\}$ and performing the Born and Markov approximations as before, we arrive at (this equation is the same in interaction and

Schrödinger pictures)

$$\begin{aligned}\frac{d\hat{\rho}_{\text{sys}}}{dt} &= -i \left[\hat{H}_{\text{sys}}(t), \hat{\rho}_{\text{sys}} \right] \\ &\quad - g^2 \sum_{\alpha\beta} \int_0^{\infty} d\tau C_{\alpha\beta}(+\tau) \left[\hat{A}_{\alpha}, \hat{A}_{\beta} \hat{\rho}_{\text{sys}} \right] \\ &\quad - g^2 \sum_{\alpha\beta} \int_0^{\infty} d\tau C_{\beta\alpha}(-\tau) \left[\hat{\rho}_{\text{sys}} \hat{A}_{\beta}, \hat{A}_{\alpha} \right] \\ &= -i \left[\hat{H}_{\text{sys}}(t) + \frac{g^2}{2i} \sum_{\alpha\beta} \sigma_{\alpha\beta} \hat{A}_{\alpha} \hat{A}_{\beta}, \hat{\rho}_{\text{sys}} \right] \\ &\quad + g^2 \sum_{\alpha\beta} \gamma_{\alpha\beta} \left[\hat{A}_{\beta} \hat{\rho}_{\text{sys}} \hat{A}_{\alpha} - \frac{1}{2} \left\{ \hat{A}_{\alpha} \hat{A}_{\beta}, \hat{\rho}_{\text{sys}} \right\} \right],\end{aligned}\tag{D2}$$

where $\sigma_{\alpha\beta} = \int_{-\infty}^{\infty} C_{\alpha\beta}(\tau) \text{sgn}(\tau) d\tau$ and $\gamma_{\alpha\beta} = \int_{-\infty}^{\infty} C_{\alpha\beta}(\tau) d\tau$. As the matrix $\gamma_{\alpha\beta}$ is positive semidefinite due to Bochner's theorem, this is a Lindblad form. We can also see that it has the completely mixed state as a stationary solution. Furthermore, the above equation is identical to the singular-coupling master equation with time-dependencies inserted *a posteriori*, compare e.g. Eq. (48) of Ref. [58].

Thus, we see that in the regime of small energy gaps in the relevant subspace, the hermitian coupling operators directly transfer to hermitian Lindblad operators that can be interpreted as a measurement performed by the environment. For undriven systems, combinations of small and large energy gaps have been treated before [61, 62], but for driven systems this has to be generalized.